JOURNAL OF MATERIALS SCIENCE 14 (1979) 1126–1140

The thermal expansion of chrysotile asbestos and its composites

C. HARWOOD*, B. YATES
Department of Pure and Applied Physics, University of Salford, UK

D. V. BADAMI
TBA Industrial Products Ltd, Rochdale, UK

The principal linear thermal expansion coefficients of chrysotile asbestos have been measured over the approximate temperature range 80 to 270 K. Implications of the results on: (i) the influence of thermal strain upon the specific heat capacity, and (ii) the temperature variation of the reduced volume dependence of the lattice vibrational frequencies have been assessed as far as available ancillary data permit. The principal linear thermal expansion coefficents of specimens prepared from composite bars consisting of phenol formaldehyde resin reinforced with chrysotile fibre in random and preferential dispositions, have also been measured over this temperature range. An appraisal of the results in the neighbourhood of ambient temperature has been undertaken in terms of a simple structural model. It transpires that a satisfactory account of the thermal expansion results for the composites is provided in terms of the thermal and elastic properties of the constituents for directions parallel to the pressing directions. The limited ancillary data available leave the principal causes of the less satisfactory agreement in directions at right angles to the pressing directions an open question, though a suggestion is advanced concerning the direction which further investigations might take in order to resolve this uncertainty.

1. Introduction

The increases of stiffness and strength which may be achieved in plastics by the addition of well dispersed fibres of asbestos are well known. A wide variety of products has been based on materials of this type for many years [1, 2], where significant improvements of performance have been achieved in complex structures at a reasonable cost. For many applications a random distribution of fibres within the matrix provides the most appropriate reinforcement, but in some cases preferential orientation is desirable in order to make the fullest use of the additional stiffness and strength available in particular directions.

The thermal expansion characteristics of the composite formed by the addition of short, structurally anisotropic fibres to a plastic matrix are strongly influenced by the volume fraction and orientation distribution of the fibres. In addition to being of general interest in a wider context, a detailed knowledge of this influence is particularly important in specialized applications of asbestos fibre-reinforced plastics where dimensional changes accompanying variations of temperature are critical.

The investigation to be described was undertaken in order to identify the main features of the temperature dependence of the thermal expansion characteristics of the basic unidirectional components of typical asbestos fibre-reinforced plastic structures, in which chrysotile fibre was employed. Because of their wider interest in a more general context, the measurements were extended to include the temperature dependences of the principal thermal expansion characteristics of the constituents of the composites, i.e. the resin and the chrysotile spelk. The account concludes with an assessment of the extent to which the thermal

*Present address: Rolls-Royce and Associates Ltd, Derby UK.

expansion characteristics of the composites may be understood in terms of the known physical properties of the constituents.

2. The specimens

2.1. Constituent materials

The resin employed as matrix in the present study was phenol formaldehyde resin, prepared from constituents including phenol and formaldehyde in the molar ratio 1:1.33. Full details of the preparation of a sample of the pure resin have been given elsewhere [3], together with accounts of measurements of its linear thermal expansion coefficient, specific heat capacity, Young's modulus and their interpretation in atomic terms. For convenience in later comparisons, the thermal expansion results for the pure resin are recapitulated in Fig. 8, after the presentation of the results for the present specimens.

The reinforcement took the form of chrysotile fibre, teased from spelk which had originated from the Cassiar mine in Northern British Columbia.

2.2. Specimens of chrysotile

The serpentine group of asbestos, of which chrysotile is the sole member, has the chemical formula $Mg_3Si_2O_5(OH)_4$. The structure is essentially a layered type, based on a pseudo-hexagonal network of SiO_4 tetrahedra forming a sheet, in which all the tetrahedra point one way. A brucite layer, $Mg(OH)_2$, is joined to the SiO_4 network in such a way that on one side two out of every three hydroxyls are replaced by oxygens at the apices of the tetrahedra. The mismatch in the dimensions of the silica and brucite sheets introduces a strain in the structure which results in curvature of the sheet with the brucite layer on the outer surface. X-ray diffraction studies [4, 5] have indicated that the resulting cylindrical lattices take the form of closed concentric cylinders, spirals and sometimes a helical arrangement. This picture has been confirmed by high resolution electron microscopy [6]. These structures and the voids between them appear to be partially filled with an amorphous magnesium silicate gel, the remaining pore volume being between approximately 4% and 5% [7, 8]. On the macroscopic scale, the symmetry is hexagonal and this necessitated thermal expansion measurements in two directions at right angles, i.e. parallel and perpendicular to the fibre direction.

Blocks of approximately 5 mm square cross-section were prepared from a large block of spelk. The specimens used for measuring thermal expansion parallel to the fibre axis were cut so as to measure 10 mm in this direction. The specimens used for measuring thermal expansion perpendicular to the fibre axis were cut into approximately 5 mm cubes. The specimens were prepared by cleaving along the fibre direction and grinding through the spelk at right angles to the fibre direction with a tungsten wire saw. Preparatory work indicated that oil lubrication and carborundum loading contaminated the product and the final grinding was performed over a period of several hours using the tungsten wire alone. Although slow, this technique ensured that the specimens so produced were free from fluffy ends, which would have reduced the accuracy to which the thermal expansion could be measured in the direction parallel to the fibres.

2.3. Composite bars

Two composite bars were produced. The first of these, henceforth known as the "random bar", was prepared by impregnating teased fibre with resin and pre-curing at 50° C for 4 h to remove excess solvent. The composite was then pressed to 3.86×10^6 N m^{-2} in a hot mould at 150° C for 30 min, by which time the resin was fully cured. A block of composite approximately 13 mm square cross-section and 100 mm long was produced, from which specimens were subsequently prepared as described in Section 2.4. For the second bar, henceforth known as the "aligned bar", teased fibre was carded and drawn, thus aligning the fibres. The carded and drawn fibre was wound in one direction only on a frame and impregnated with resin. The felt thus produced was pre-cured as above and then cut into strips parallel to the alignment direction in order to fit the mould. The strips were packed into the hot mould and pressed to 3.86×10^6 N m^{-2} at 150° C for 30 min, as above. A rectangular block of composite the same size as the first was produced which had principal axes: (i) parallel to the carding direction (designated the x-direction), (ii) parallel to the pressing direction (designated the z-direction) and (iii) perpendicular to both of these directions (designated the y-direction). Specimens were prepared from this bar as described in Section 2.4. The co-ordinate system described above was also taken for the "random composite", although the x- and y-directions were identical.

TABLE I The specimens

Specimen designation	Description of specimen	Direction of thermal expansion measurements	Fibre volume (%)	Void content (%)
1	Chrysotile spelk	Parallel to fibres		
2	Chrysotile spelk	Perpendicular to fibres		
3	Random composite	Parallel to pressing direction	55.9	1.4
4	Random composite	Perpendicular to pressing direction	55.9	1.4
5	Aligned composite	Parallel to pressing direction	55.3	1.0
6	Aligned composite	Perpendicular to pressing direction and parallel to carding direction	55.3	1.0
7	Aligned composite	Perpendicular to pressing direction and perpendicular to carding direction	55.3	1.0

As part of the characterization of the fibres employed in the random bar, chrysotile flock was gently teased into a very loose configuration, following which the diameters and lengths of 200 fibres were measured with the aid of optical magnification and recording techniques. The average diameter, d, 5.44×10^{-2} mm, and the average length, l, 3.3 mm, gave an aspect ratio $l/d = 60.7$. The averages of corresponding determinations on 200 fibres of carded and drawn asbestos, as employed in the aligned bar, were $d = 3.06 \times 10^{-2}$ mm, $l = 3.9$ mm, giving $l/d = 127$. Wafers measuring approximately 50 mm × 10 mm × 1 mm were cut parallel and perpendicular to the z-direction of the random composite and in the x–y and x–z planes of the aligned composite. These were mounted, in turn, in an X-ray texture goniometer, which was employed to determine the fibre orientations in the planes of the wafers. The output from the diffracted beam was displayed on a chart recorder, from which the corresponding orientation distributions of the fibres were calculated after correcting for the effects of the background radiation.

2.4. Specimen preparation, characterization and measurement

Rejecting material from the boundaries of the blocks and concentrating upon the more nearly void-free regions, sets of three specimens were prepared, approximately 10 mm long, corresponding to the directions summarized in Table I. This was achieved using a diamond slitting wheel lubricated with water to prevent local heating. The surfaces of the specimens were polished to remove any strained surface layers using fine emery paper and polishing paper.

Fibre volume fractions of approximately 50% were aimed for in the production of the bars. The actual compositions were determined from the weight loss incurred by burning off the resin from control specimens. As part of this evaluation, subsidiary heating investigations were undertaken with pure chrysotile in order to determine the fraction of the above weight reduction which had resulted from loss of hydroxyl groups. The final figures for the fibre volume fractions of the random and aligned bars were 55.9% and 55.3%, respectively. These figures were employed, together with the known densities of the chrysotile and resin, to calculate the void content of the random bar as 1.4% and that of the aligned bar as 1.0%. The better figure for the aligned bar is believed to result from the improved packing of aligned fibres, compared with random fibres.

The Fizeau interferometric apparatus employed for the measurements has been described elsewhere [3]. A lack of reproducibility, which was later shown to be associated with a variable water content, was reported in the thermal expansion work on the pure resin [3]. No such effects were encountered in the present work, in which it is believed that the fibres might have provided channels through which trapped water could escape from the resin matrix.

3. Thermal expansion results

The primary data resulting from the measurements are displayed graphically in Figs. 1 to 7 in order to convey some idea of the precision to which they were measured, in addition to being summarized in Table II in smoothed form for convenience. The value of figures for absolute accuracy expressed in percentage form is questionable when applied to

TABLE II Smoothed values of the linear thermal expansion coefficients α of the specimens described in Table I

T (K)	α (K^{-1}) for the specimens numbered below						
	1 $\times 10^{-6}$	2 $\times 10^{-6}$	3 $\times 10^{-6}$	4 $\times 10^{-6}$	5 $\times 10^{-6}$	6 $\times 10^{-6}$	7 $\times 10^{-6}$
80	−0.70		9.31	2.49	8.98	0.56	5.45
90	−0.35	4.40	10.08	2.88	9.70	0.80	5.99
100	−0.03	5.06	10.83	3.24	10.40	1.02	6.49
110	0.26	5.66	11.55	3.57	11.10	1.24	6.98
120	0.54	6.26	12.22	3.88	11.75	1.45	7.45
130	0.80	6.83	12.87	4.18	12.35	1.66	7.89
140	1.04	7.38	13.44	4.46	12.92	1.85	8.31
150	1.28	7.89	14.00	4.71	13.46	2.04	8.70
160	1.50	8.40	14.50	4.96	13.95	2.23	9.07
170	1.72	8.86	14.91	5.20	14.40	2.40	9.40
180	1.93	9.32	15.39	5.44	14.78	2.56	9.70
190	2.12	9.74	15.90	5.66	15.10	2.71	9.97
200	2.31	10.12	16.52	5.87	15.50	2.89	10.25
210	2.50	10.48	17.20	6.11	15.94	3.09	10.55
220	2.68	10.82	18.00	6.36	16.44	3.29	10.86
230	2.85	11.14	18.90	6.64	17.00	3.50	11.18
240	3.02	11.45	19.76	6.91	17.68	3.73	11.52
250	3.18	11.74	20.57	7.21	18.40	3.97	11.87
260	3.35	12.03	21.33	7.51	19.21	4.21	12.23
270	3.50	12.30	22.06	7.82	20.07		12.60

linear thermal expansion coefficients which pass through zero. A better idea of the capabilities of the apparatus in absolute terms may be gained by studying its performance when it was used to examine specimens of standard NBS fused silica SRM 739 [9], for which smoothed data have been issued by the National Bureau of Standards.

The only relevant earlier results found were for chrysotile. These consist of a value for the linear thermal expansion coefficient, direction not specified, of $50 \times 10^{-6}\ K^{-1}$ [10], and an estimated value for the volume thermal expansion coefficient of $80 \times 10^{-6}\ K^{-1}$ [11]. Meaningful comments upon these results in relation to the results of the present work are prevented by an absence of knowledge which would permit a detailed comparison of the specimens employed on the three occasions.

4. Discussion

4.1. Chrysotile

A combined knowledge of the specific heat capacity, linear thermal expansion coefficients and elastic constants of a solid, over a wide range of temperature, permit the calculation of vibrational properties which are directly related to its frequency spectrum. The specific heat capacity occupies a particularly important place in this group, but a knowledge of the principal linear thermal expansion coefficients allows further information to be gleaned.

4.1.1. The principal linear thermal expansion coefficients

Previous experience of the thermal expansion characteristics of pyrolytic graphite [12] and boron nitride [13], both of which possess anisotropic structures, indicates that two features in the results for the linear thermal expansion coefficient parallel to the fibres of the chrysotile spelk, $\alpha_{\parallel}^{f}$, displayed in Fig. 1, deserve comment. The low value of $\alpha_{\parallel}^{f}$ suggests tight binding between the atoms within the planes and this is consistent with the high Young's modulus in the fibre direction. At the lowest temperatures of the investigation $\alpha_{\parallel}^{f}$ assumes negative values. This behaviour is consistent with a high density of transverse modes of vibration, which is favoured by open structures [14, 15]. This observation accords with known features of the structure within the planes. The sign and temperature dependence of the linear thermal expansion coefficient perpendicular to the fibres, $\alpha_{\perp}^{f}$, contain no unusual features. On the other hand, the atomic structure of chrysotile might be expected to have comparatively weak forces between the silica and brucite layers, favouring a comparatively high value of $\alpha_{\perp}^{f}$, whereas in fact $\alpha_{\perp}^{f}$ is not very

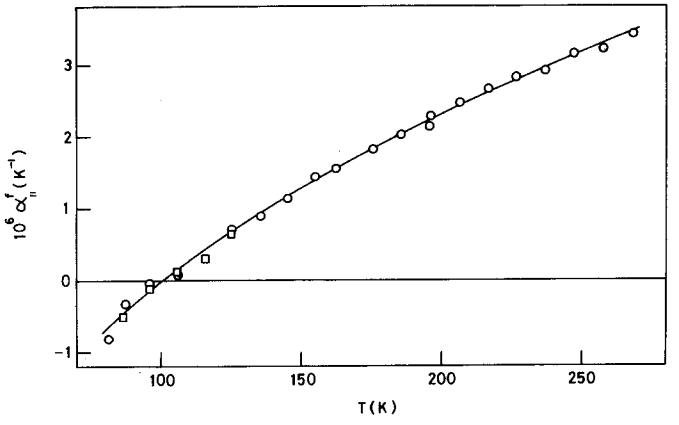

Figure 1 The linear thermal expansion coefficient $\alpha_{\parallel}^{f}$ of chrysotile asbestos, in a direction parallel to the fibres (specimens 1): ○ 1st series, □ 2nd series of results.

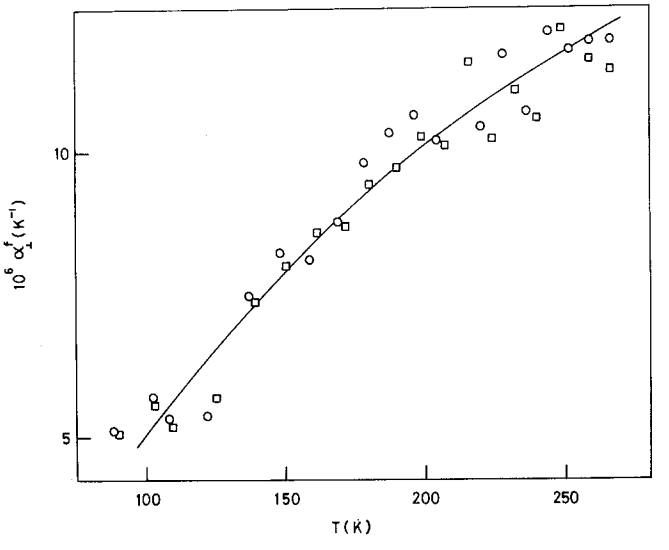

Figure 2 The linear thermal expansion coefficient $\alpha_{\perp}^{f}$ of chrysotile asbestos, in a direction perpendicular to the fibres (specimens 2): ○ 1st series, □ 2nd series of results.

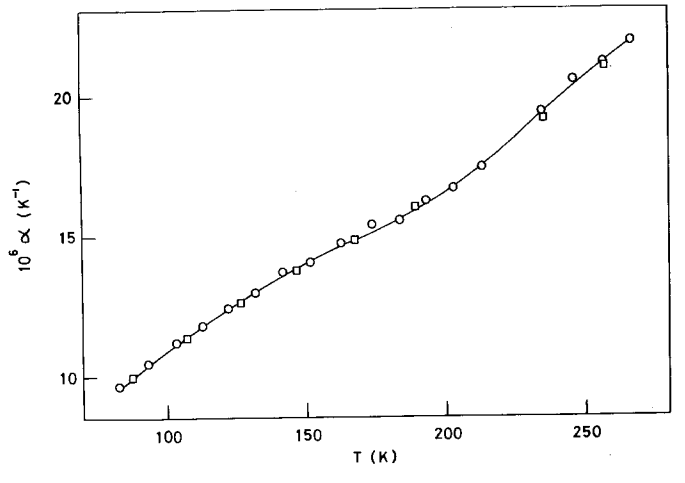

Figure 3 The linear thermal expansion coefficient α of specimens 3: ○ 1st series, □ 2nd series of results.

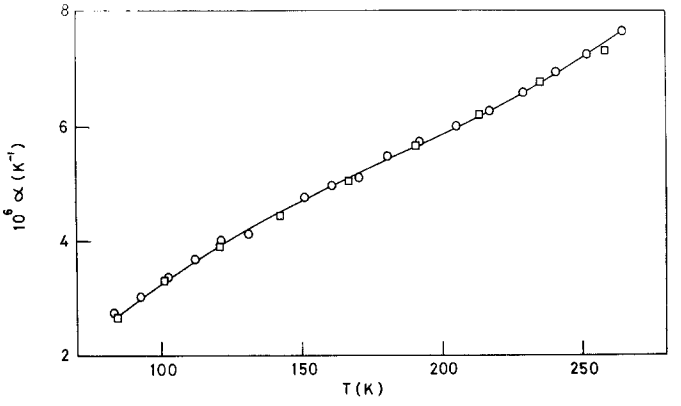

Figure 4 The linear thermal expansion coefficient α of specimens 4: ○ 1st series, □ 2nd series of results.

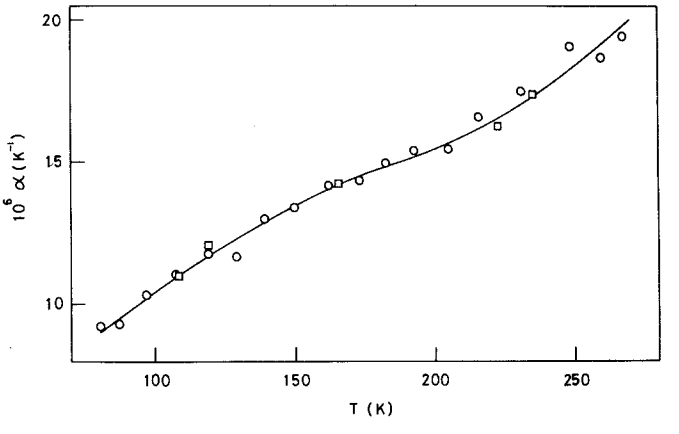

Figure 5 The linear thermal expansion coefficient α of specimens 5: ○ 1st series, □ 2nd series of results.

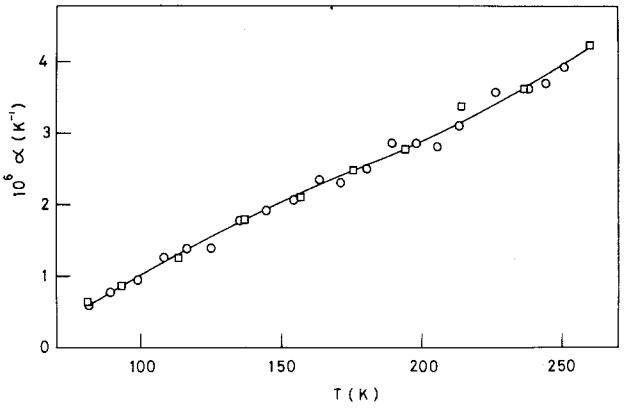

Figure 6 The linear thermal expansion coefficient α of specimens 6: ○ 1st series, □ 2nd series of results.

much bigger than $\alpha_{\parallel}^{f}$. It seems at least possible that the voids within the structure are providing accommodation for some of the thermal expansion perpendicular to the fibres. This could be checked by measuring $\alpha_{\perp}^{f}$ using an X-ray technique, when distinctly higher values of $\alpha_{\perp}^{f}$ should be found if this interpretation is correct. Alternatively the magnitude of $\alpha_{\perp}^{f}$ might be limited by strain within the chrysotile lattice, resulting from the coiled structure.

4.1.2. The influence of thermal strain

In order to calculate lattice vibrational properties of a solid from its specific heat capacity it is necessary to calculate the value at constant strain C_{η} from the value which is measured at constant stress C_{t}. An absence of knowledge of the temperature dependence of the isothermal bulk modulus of elasticity χ_T prevents this, but some progress is possible with the aid of the thermodynamic equation

Figure 7 The linear thermal expansion coefficient α of specimens 7: ○ 1st series, □ 2nd series of results.

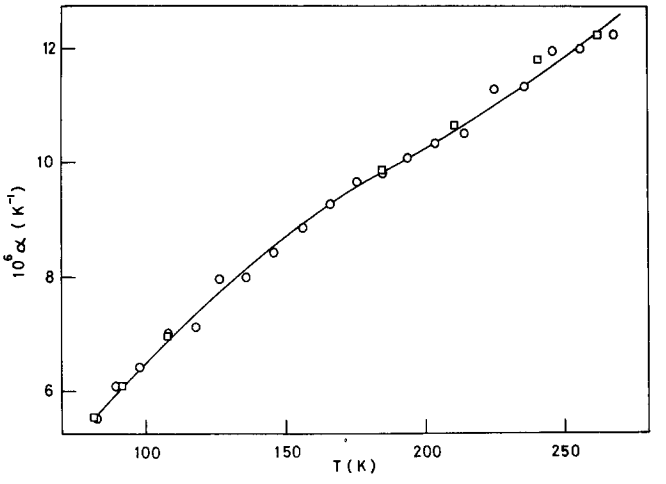

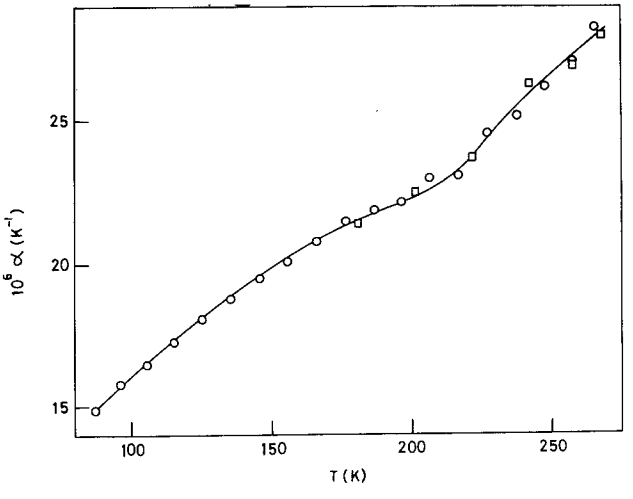

Figure 8 The linear thermal expansion coefficient α of (1 : 1.33) phenol formaldehyde resin: ○ run 2, □ run 3 of Harwood *et al.* [3].

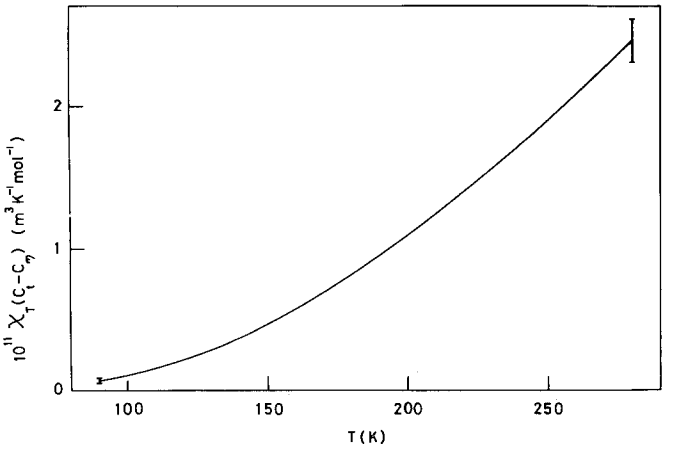

Figure 9 The difference between the specific heat capacities of chrysotile asbestos at constant stress C_t and constant strain C_η expressed in reduced form, in which χ_T is the isothermal compressibility. Experimental uncertainties at the limits of the temperature range are depicted by the vertical lines.

$$\chi_T (C_t - C_\eta) = V\beta^2 T, \quad (1)$$

in which β is the volume thermal expansion coefficient and V, T have their usual meanings. The density of chrysotile was measured by Pundsack [7], most of whose measurements were made on specimens from a supply of Danville Crude from Canada. Values ranging between 2.53×10^3 and 2.58×10^3 kg m^{-3} were reported and a room temperature value of 2.56×10^3 kg m^{-3} was assumed in the present work. Employing this in association with values of $\beta = \alpha_{\|}^f + 2\alpha_{\perp}^f$ produced

the results for the functions $\chi_T (C_t - C_\eta)$ displayed in smoothed form in Fig. 9. The only elastic constant for chrysotile which appears to have been measured is the Young's modulus in a direction parallel to the fibres, at room temperature [2, 11]. Taking this to give an order of magnitude for the bulk modulus allowed $(C_t - C_\eta)$ to be estimated at between 1% and 2% in the neighbourhood of room temperature. Since $(C_t - C_\eta)$ diminishes with fall of temperature to zero at absolute zero, it is clear that vibrational properties calculated from C_t rather than C_η will not be seriously in error on this account.

4.1.3. The specific heat capacity

The Debye characteristic temperature of a simple solid is particularly useful in leading to the moments of its vibrational spectrum and their volume dependence. In the case of more complex solids, in which different types of vibration are open to groups of atoms within the assembly, progress is still possible provided that the individual spectra do not overlap. The structure of the chrysotile molecule is so complex, however, that significant progress in employing thermodynamic data in this way could only be made if the detailed elasticity data were available as functions of temperature, and even then it is doubtful whether more than gross features would be discerned. In view of these limitations a characteristic temperature assuming $3nN$ vibrations per mole has been calculated, in which n is the atomicity and N is Avogadro's number. This function, which refers to the resultant spectrum, is displayed in Fig. 10. Apart from being linear in temperature over a wide range it displays no unusual features and the limited value of the averaged thermodynamic functions to which it opens the way was not considered sufficient to justify the additional calculation which would have been involved in their evaluation. Of the experimental specific heat capacities examined [16, 17], the well documented results of King *et al.* [16] were adopted for the present purpose. These workers measured the low temperature specific heat capacity of a natural sample of chrysotile which was considered to be 94% pure. Corrections were applied for excess water and other impurities, which were assumed to consist mainly of silicates, aluminates and ferrites, following which the results were believed to be accurate in an absolute sense to within 0.5%.

4.1.4. The Grüneisen parameters

Defining a Grüneisen parameter $\gamma_{mean} = \beta V / C_t \chi_s$, χ_s being the adiabatic compressibility, the quantity $\chi_s \gamma_{mean}$ has been evaluated as a function of temperature. This function is plotted in Fig. 11, from which it may be seen that the increase with diminishing temperature lies outside the nominal limits attributed to experimental uncertainty. Speculation as to the likely temperature dependence of γ_{mean} would be of little value in the absence of a knowledge of the temperature dependence of the compressibility of a material having a structure resembling that of chrysotile. More detailed information concerning the volume dependences of the frequencies of the lattice

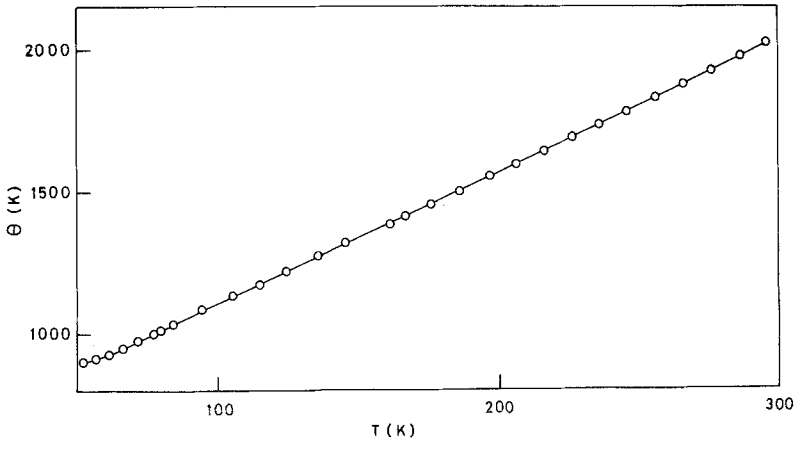

Figure 10 The Debye characteristic temperature θ of chrysotile asbestos, calculated assuming $18N$ vibrations per mole and neglecting the correction $(C_t - C_\eta)$. Experimental uncertainties are smaller than the diameters of the circles depicting the experimental results.

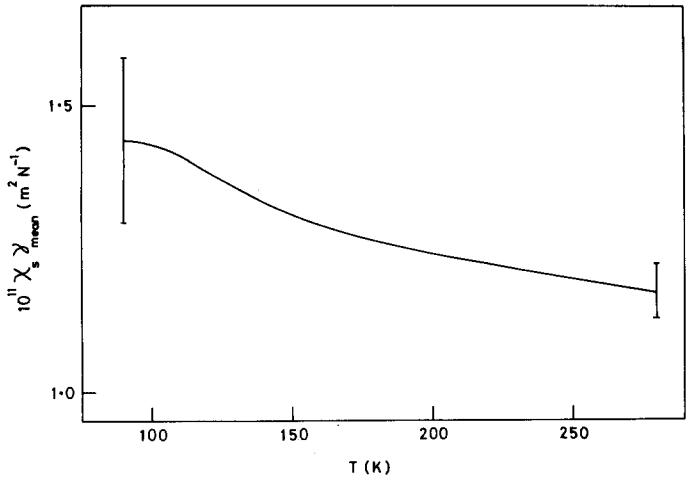

Figure 11 Reduced mean Grüneisen parameter of chrysotile asbestos spelk as a function of temperature, in which nominal uncertainty limits of ± 10% are displayed at the limits of the temperature range.

vibrations would be possible with a knowledge of the elastic constants c_{11}, c_{12}, c_{13} and c_{33} as functions of temperature. Together with the heat capacity and thermal expansion data, these would permit the calculation of the Grüneisen parameters

$$\gamma_{\parallel} = \frac{V}{C_t}\left[2c_{13}\,\alpha_{\perp}^{f} + c_{33}\,\alpha_{\parallel}^{f}\right] \qquad (2)$$

and

$$\gamma_{\perp} = \frac{V}{C_t}\left[(c_{11} + c_{12})\,\alpha_{\perp}^{f} + c_{13}\,\alpha_{\parallel}^{f}\right], \qquad (3)$$

which may be associated with directions parallel and perpendicular to the fibre direction [18].

4.1.5. Additional considerations

There is some interest in the temperature dependence of the ratio of the principal linear thermal expansion coefficients $\alpha_{\parallel}^{f}/\alpha_{\perp}^{f}$, displayed in Fig. 12, through Equations 2 and 3. Examination of these equations reveals that:

when

$$\gamma_{\parallel} = -\gamma_{\perp},$$

$$\frac{\alpha_{\parallel}^{f}}{\alpha_{\perp}^{f}} = \frac{2c_{13} - (c_{11} + c_{12})}{c_{13} + c_{33}}, \qquad (4)$$

when

$$\gamma_{\perp} = 0,$$

$$\frac{\alpha_{\parallel}^{f}}{\alpha_{\perp}^{f}} = -\left(\frac{c_{11} + c_{12}}{c_{13}}\right) \qquad (5)$$

and when

$$\gamma_{\parallel} = \gamma_{\perp},$$

$$\frac{\alpha_{\parallel}^{f}}{\alpha_{\perp}^{f}} = \frac{2c_{13} - (c_{11} + c_{12})}{c_{13} - c_{33}}. \qquad (6)$$

The temperatures at which these three relationships hold for the true values of $\gamma_{\parallel}$ and $\gamma_{\perp}$ at these temperatures and the corresponding values of

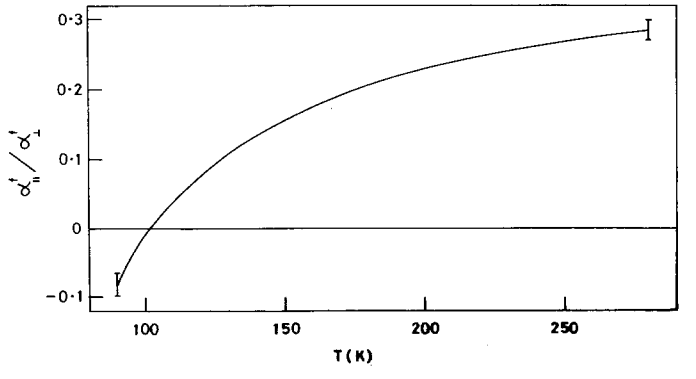

Figure 12 The ratio of the principal linear thermal expansion coefficients of chrysotile asbestos, in which $\alpha_{\parallel}^{f}$ and $\alpha_{\perp}^{f}$ denote values parallel and perpendicular to the fibres respectively. Experimental uncertainties at the limits of the temperature range are depicted by the vertical lines.

$\alpha_{\|}^{f}/\alpha_{\perp}^{f}$ are clearly inter-related. Thus, if experimentally determined temperature dependent values of c_{13} or $(c_{11} + c_{12})$ were to be substituted into Equation 2 and/or Equation 3, as appropriate, reiterative adjustment of the outstanding elastic constant(s) to achieve self-consistency among Equations 2 to 6 should provide a means of determining them more precisely at these temperatures.

4.2. The composites

4.2.1. Preliminary remarks

A number of attempts to predict the principal linear thermal expansion coefficients of unidirectional composites, consisting of matrices reinforced with continuous fibres, have appeared over the years [e.g. 19–21]. Corresponding to the direction parallel to the fibres these all produced the same mathematical expression, but for the direction at right angles different results were predicted. Halpin and Pagano [22] went on to consider the in-plane thermal expansion characteristics of symmetrically balanced angle ply laminates and Pagano [23] later considered the out-of-plane case. The results of a recent study of the thermal expansion characteristics of a series of carbon fibre-reinforced plastics [24, 25] were analysed with the aid of the ideas contained in these treatments. Within restrictions imposed by the relevant physical data available for the constituents it was concluded that proper application of the models served to give a reasonably self-consistent account of the observations.

The thermal expansion of short fibre-reinforced matrices has been dealt with less comprehensively than the corresponding case involving continuous fibres. Idealized cases of two-dimensional matrices containing randomly oriented short fibres and perfectly aligned short fibres have been considered [26, 27] and the case of preferential alignment in a two-dimensional matrix has been investigated [28] with the aid of a laminate analogy. Formulae have also been derived to predict the effective elastic properties of a composite containing randomly oriented fibres [29, 30] but the case of the preferential alignment of short fibres in three dimensions does not appear to have been considered.

4.2.2. Qualitative observations

Before examining the extent to which the thermal expansion characteristics of the composites may be understood in terms of the linear thermal expansion coefficients and elastic constants of the constituents, a brief qualitative examination of the salient features of the results is worthwhile.

4.2.2.1. Specimens 3 and 4. One of the scans undertaken with the X-ray goniometer indicated that the effect of applying pressure to the resin containing a random distribution of fibres, during the preparation of the random bar, was to give the fibres a preferential alignment perpendicular to the pressing direction. The linear thermal expansion coefficient of specimens 3 might, therefore, be expected to lie between those of the pure resin and specimens 2, that of specimens 4 might be expected to lie between those of the pure resin and specimens 1, and that of specimens 3 might be expected to exceed that of specimens 4. Examination of Figs. 1 to 4 and 8 reveals that all these expectations are borne out. Fig. 8 reveals a deviation from the monotonic variation of the linear thermal expansion coefficient of the resin with temperature over the approximate range 180 to 250 K, the effects of which are visible in the results for the composite specimens 3 and 4, displayed in Figs. 3 and 4, respectively.

4.2.2.2. Specimens 5, 6 and 7. Turning to specimens prepared from the aligned bar, examination of the X-ray texture goniometer scans revealed that the effect of carding was to give the fibres a preferential alignment in the x-direction, while the effect of pressure on the composite mixture had been to give the fibres a preferential alignment perpendicular to the z-direction, as before. It is, therefore, to be expected that the linear thermal expansion coefficient in the z-direction (specimens 5) should exceed that in the y-direction (specimens 7) which, in turn, should exceed that in the x-direction (specimens 6). In addition, the linear thermal expansion coefficient of specimens 5 might be expected to lie between those of the pure resin and specimens 2, while those of specimens 6 and 7 should both lie between those of the pure resin and specimens 1. Examination of the relevant figures shows that all these expectations are borne out and, as in the case of results for specimens 3 and 4, the results for the specimens prepared from the aligned bar contain signs of the deviation from monotonic behaviour displayed by the results for the pure resin.

4.2.3. Structure representation

In addition to being mathematically complex, a rigorous treatment of the case of a preferential alignment in three dimensions would be of little more than academic interest in the present case because of the limited elastic constant data available. The following approach was developed in an attempt to explore the extent to which an approximate understanding of the results for the composites could be gained from the limited experimental data available.

Suppose the composite may be considered to be constructed from a series of elemental blocks of resin, each of which contains one fibre along a central axis. The complete assembly, containing random or preferential alignment, may then be supposed to be made up by stacking the blocks in the appropriate sequence. The thermal expansion characteristics of the blocks in directions parallel and perpendicular to the fibres, $\alpha_{\parallel}^{c}$ and $\alpha_{\perp}^{c}$ respectively, may be calculated using Halpin's modification [27] of Schapery's equation [20] for a short fibre-reinforced composite, assuming a fibre volume fraction and aspect ratio equal to that of the macroscopic specimens. Suppose that the fibre axis of a block lies along direction OA in Fig. 13, in which the element of solid angle between directions θ, $\theta + d\theta$, and $\phi, \phi + d\phi$ is clearly $\sin\theta d\theta d\phi$. If we now introduce a distribution function $I(\theta, \phi)$, which is proportional to the number of fibres per unit solid angle having orientation (θ, ϕ) in unit volume, then the number of fibres per unit volume directed into the element of solid angle defined above will be proportional to $I(\theta, \phi) \sin\theta d\theta d\phi$.

A polar plot of the distribution function might be expected to resemble Fig. 14, in which $OA = I(\theta, \phi)$. Fibre distributions measured with the X-ray texture goniometer provide the contours B′A′C and B′BB″, but in order to express the linear thermal expansion coefficients in the principal directions Ox, Oy and Oz in terms of the corresponding properties of the elemental blocks, it is necessary to know how the shape of the contours B′A′C and B′BB″ vary as they are rotated about Oz and Ox respectively. The empirical relation

$$(OA' - OA) = (OB' - OB)\sin\theta \qquad (7)$$

satisfies the boundary conditions that $(OA' - OA)$ should have a maximum value $(OB' - OB)$ when $\theta = \pi/2$ and a minimum value 0 when $\theta = 0$. Ex-

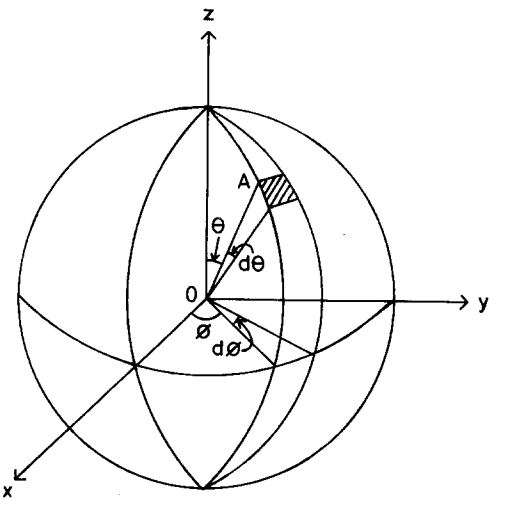

Figure 13 Illustration of the angular parameters employed in calculating the thermoelastic properties of the composites.

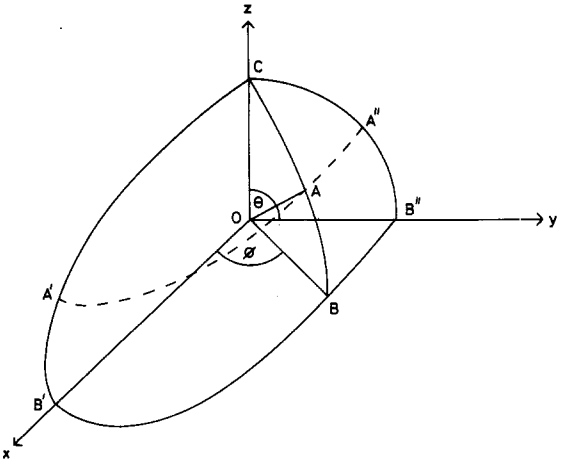

Figure 14 A polar plot of the function $I(\theta, \phi)$, illustrating the preferential orientations of the fibres.

pressed in terms of the distribution function this becomes

$$I(\theta, \phi) = I(\theta, 0) - \left[I\left(\frac{\pi}{2}, 0\right) - I\left(\frac{\pi}{2}, \phi\right)\right] \sin\theta. \qquad (8)$$

4.2.4. Thermal expansion characteristics

4.2.4.1. Formal considerations. If the contribution to the linear thermal expansion coefficient in the direction Oz, α_z^c, from fibres having their axes oriented at (θ, ϕ) to Oz is proportional to the number of such fibres, $(dN)_{\theta,\phi}$ then

$$\alpha_z^c = \frac{\sum_{\theta,\phi} (\alpha_z^c)_{\theta,\phi} (dN)_{\theta,\phi}}{\sum_{\theta,\phi} (dN)_{\theta,\phi}} . \qquad (9)$$

We saw earlier that $(dN)_{\theta,\phi} \propto I(\theta, \phi) \sin\theta \, d\theta \, d\phi$. Substituting this, together with the result

$$(\alpha_z^c)_{\theta,\phi} = \alpha_\parallel^c \cos^2\theta + \alpha_\perp^c \sin^2\theta \tag{10}$$

into Equation 9 produces the expression

$$\alpha_z^c = \frac{\int_0^\pi \int_0^\pi I(\theta,\phi)\,[\alpha_\parallel^c \cos^2\theta + \alpha_\perp^c \sin^2\theta]\,\sin\theta \, d\theta d\phi.}{\int_0^\pi \int_0^\pi I(\theta,\phi)\sin\theta \, d\theta d\phi}. \tag{11}$$

Substituting for $I(\theta, \phi)$ from Equation 8, this becomes

$$\alpha_z^c = \frac{\int_0^\pi \int_0^\pi \left\{I(\theta,0) - \left[I\left(\frac{\pi}{2},0\right) - I\left(\frac{\pi}{2},\phi\right)\right]\sin\theta\right\}\{\alpha_\parallel^c \cos^2\theta + \alpha_\perp^c \sin^2\theta\}\sin\theta \, d\theta d\phi}{\int_0^\pi \int_0^\pi \left\{I(\theta,0) - \left[I\left(\frac{\pi}{2},0\right) - I\left(\frac{\pi}{2},\phi\right)\right]\sin\theta\right\}\sin\theta \, d\theta d\phi}. \tag{12}$$

Evaluating the various terms in this expression finally leads to the following result for the linear thermal expansion coefficient of the aligned composite in the direction Oz:

$$\alpha_{az}^c = \frac{\alpha_\parallel^c \int_0^\pi I(\theta,0)\sin\theta\cos^2\theta \, d\theta + \alpha_\perp^c \int_0^\pi I(\theta,0)\sin^3\theta \, d\theta + [(\alpha_\parallel^c + 3\alpha_\perp^c)/8]\left\{\int_0^\pi I\left(\frac{\pi}{2},\phi\right)d\phi - \pi I\left(\frac{\pi}{2},0\right)\right\}}{\int_0^\pi I(\theta,0)\sin\theta \, d\theta + \left\{\int_0^\pi I\left(\frac{\pi}{2},\phi\right)d\phi - \pi I\left(\frac{\pi}{2},0\right)\right\}\Big/2}. \tag{13}$$

In the case of the random composite $I(\pi/2, \phi) = I(\pi/2, 0)$ and the terms in curly brackets in Equation 13 become zero, giving

$$\alpha_{rz}^c = \frac{\alpha_\parallel^c \int_0^\pi I(\theta,0)\sin\theta\cos^2\theta \, d\theta + \alpha_\perp^c \int_0^\pi I(\theta,0)\sin^3\theta \, d\theta}{\int_0^\pi I(\theta,0)\sin\theta \, d\theta} \tag{14}$$

for the linear thermal expansion coefficient of the random composite in the direction Oz.

Considering next the direction Ox, the expression for the linear thermal expansion coefficient which corresponds with Equation 9 is

$$\alpha_x^c = \frac{\sum_{\theta,\phi} (\alpha_x^c)_{\theta,\phi}\,(dN)_{\theta,\phi}}{\sum_{\theta,\phi} (dN)_{\theta,\phi}}, \tag{15}$$

where $(\alpha_x^c)_{\theta,\phi}$ is the contribution to the linear thermal expansion coefficient of the composite in the direction Ox, from fibres having orientation (θ, ϕ). Denoting the angle between OA and Ox by $\hat{x}$,

$$(\alpha_x^c)_{\theta,\phi} = \alpha_\parallel^c \cos^2\hat{x} + \alpha_\perp^c \sin^2\hat{x}, \tag{16}$$

in which $\cos\hat{x} = \sin\theta\cos\phi$. Substituting these results in Equation 5 and employing the result $(dN)_{\theta,\phi} \propto I(\theta, \phi)\sin\theta \, d\theta \, d\phi$ finally leads to

$$\alpha_{ax}^c = \frac{\left[\frac{(\alpha_\parallel^c - \alpha_\perp^c)}{2}\int_0^\pi I(\theta,0)\sin^3\theta \, d\theta + \alpha_\perp^c \int_0^\pi I(\theta,0)\sin\theta \, d\theta + \frac{3}{8}(\alpha_\parallel^c - \alpha_\perp^c)\left\{\int_0^\pi I\left(\frac{\pi}{2},\phi\right)\cos^2\phi \, d\phi - \frac{\pi}{2} I\left(\frac{\pi}{2},0\right)\right\} + \frac{\alpha_\perp^c}{2}\left\{\int_0^\pi I\left(\frac{\pi}{2},\phi\right)d\phi - \pi I\left(\frac{\pi}{2},0\right)\right\}\right]}{\int_0^\pi I(\theta,0)\sin\theta \, d\theta + \frac{1}{2}\left\{\int_0^\pi I\left(\frac{\pi}{2},\phi\right)d\phi - \pi I\left(\frac{\pi}{2},0\right)\right\}} \tag{17}$$

for the linear thermal expansion coefficient of the aligned composite in the direction Ox. In the case of the corresponding random composite $I(\pi/2, \phi) = I(\pi/2, 0)$, as before, and the terms in curly brackets become zero, leaving

$$\alpha^c_{rx} = \alpha^c_\perp + \left[\frac{\int_0^\pi I(\theta,0)\sin^3\theta \mathrm{d}\theta}{2\int_0^\pi I(\theta,0)\sin\theta \mathrm{d}\theta}\right](\alpha^c_\parallel - \alpha^c_\perp) \quad (18)$$

for the linear thermal expansion coefficient of the random composite in directions perpendicular to Oz.

Employing a similar procedure to the case of the direction Oy leads to an expression identical to Equation 17 apart from the term

$$\int_0^\pi I\left(\frac{\pi}{2}, \phi\right)\cos^2\phi \mathrm{d}\phi$$

in the numerator, which is replaced by

$$\int_0^\pi I\left(\frac{\pi}{2}, \phi\right)\sin^2\phi \mathrm{d}\phi.$$

4.2.4.2. Numerical appraisal. In order to be able to assess the standing of the foregoing equations for the principal linear thermal expansion coefficients of the two composites it was first necessary to calculate $\alpha^c_\parallel$ and $\alpha^c_\perp$ for the elemental blocks. Because a number of the quantities required for these calculations were known at room temperature only, the assessment had to be limited to this temperature. As a preliminary, the Young's modulus of an elemental block in a direction parallel to the fibre, $E^c_\parallel$, was first calculated in the manner described by Halpin [27]. In this calculation the values of the aspect ratios and fibre volume fractions reported in 2.4 were employed, together with a value of $E_m = 3.5\,\mathrm{GN\,m^{-2}}$ for the Young's modulus of the resin [3] and $E^f_\parallel = 145\,\mathrm{GN\,m^{-2}}$ for the Young's modulus of the fibres in a direction parallel to their length [2]. In this way $E^c_\parallel$ was estimated at $72.6\,\mathrm{GN\,m^{-2}}$ in the case of the random composite and $72.8\,\mathrm{GN\,m^{-2}}$ in the case of the aligned composite. These figures were employed in the subsequent calculations (following [27]) of $\alpha^c_\parallel = 4.18 \times 10^{-6}\,\mathrm{K^{-1}}$, $\alpha^c_\perp = 23.5 \times 10^{-6}\,\mathrm{K^{-1}}$ in the case of the random composite and $\alpha^c_\parallel = 4.18 \times 10^{-6}\,\mathrm{K^{-1}}$, $\alpha^c_\perp = 23.6 \times 10^{-6}\,\mathrm{K^{-1}}$ in the case of the aligned composite. Small extrapolations of the experimental data were necessary in order to arrive at values close to room temperature for the linear thermal expansion coefficients of the resin ($\alpha_m = 29.4 \times 10^{-6}\,\mathrm{K^{-1}}$) and of the fibres in a direction parallel to their length ($\alpha^f_\parallel = 3.55 \times 10^{-6}\,\mathrm{K^{-1}}$). In the absence of experimental data, comparative considerations finally led to the adoption of values for the Poisson's ratio $\nu_m = 0.37$ [3] for the resin and $\nu^f_{\parallel\perp} = 0.30$ for the fibre. The uncertainty turns out to be the greater in the case of the term which has the lesser influence in subsequent calculations, $\nu^f_{\parallel\perp}$. A detailed consideration of the uncertainties involved in the estimation of the above values of $\alpha^c_\parallel$ and $\alpha^c_\perp$ indicates that these should not exceed a few per cent.

TABLE III Principal linear thermal expansion coefficients ar room temperature

Specimen designation	Linear thermal expansion coefficient	Experimental (extrapolated) result $\times 10^{-6}$	Calculated result $\times 10^{-6}$
3	α_{rz}	23	23.5
4	α_{rx}	8	16
5	α_{az}	21	20
6	α_{ax}	5	20
7	α_{ay}	13	12

Applying these results in the appropriate sequence to Equations 13, 14, 17 and 18, together with normalized graphical integrations of the terms in $I(\theta, \phi)$, evaluated with the aid of the X-ray texture goniometer analyses, finally led to the calculated values of α_{rz}, α_{rx}, α_{az}, α_{ax}, α_{ay} summarized in Table III. The (extrapolated) smoothed experimental values are also collected in this table for comparison. In view of the unavoidable uncertainties associated with the extrapolations of the experimental results and the estimated uncertainties in the calculated results, the figures (with one exception) have been rounded off to the nearest part in 10^{-6}. It is clear that agreement between measured and calculated results is good when dealing with directions in which the resin plays the dominant role, i.e. directions approximately perpendicular to the fibres (specimens 3, 5 and 7). It is worse when the fibres are playing an increasingly important part in determining the thermal expansion behaviour (specimen 4) and worst of all when the fibres are dominating the behaviour, i.e. in a direction with which the fibres are quite well aligned (specimen 6). This result is in keeping with a comparable observation on unidirectional continuous carbon

fibre reinforced plastics [24], in which attention was drawn to the large percentage changes in the quantity corresponding to α_{ax} which resulted from small percentage changes in $E_{\parallel}^{f}$. Ignoring a number of elastic constants of the fibres, assessing others and resting heavily upon the empirical Equation 7, the present analysis is in no sense rigorous. For this reason hypothetical adjustments of $E_{\parallel}^{f}$ would be of little value in the present instance.

5. Conclusions

Measurements of the principal linear thermal expansion coefficients of chrysotile asbestos have been employed, together with ancillary data, to gain a preliminary insight into some of the vibrational characteristics of this mineral. In association with earlier thermal expansion measurements conducted upon phenol formaldehyde resin, which formed the matrix of composites reinforced by chrysotile fibres, the results have been employed in an appraisal of thermal expansion measurements conducted upon specimens prepared from the composites.

Investigations designed to produce thermal expansion data for composites, which are subsequently subjected to analysis on the basis of a collection of plausible assumptions, are frequently beset by problems arising from insufficient ancillary experimental data. This is particularly true when the reinforcing agent takes the form of structurally anisotropic fibres. Of these, chrysotile fibres are less well standardized than many, partly because of variations of composition associated with their different origins, partly because of impurities and partly because of a variable aspect ratio. Their straightness in a composite cannot be assured, fibre agglomeration cannot be avoided and a perfectly uniform fibre volume fraction cannot be achieved throughout the composite. These difficulties were recognized at the outset and a high degree of concord between observations and predictions based upon a simple structural model was not expected. In spite of these limitations the model has given encouraging results in the direction of low alignment density of the fibres. A next logical step in the development of an improved understanding of the dilatational behaviour of short fibre-reinforced plastics in a direction parallel to the fibres could take the form of an investigation involving better characterized fibres, which had a more nearly standard composition and a more uniform dispersion. Isotropic fibres would be particularly suitable, lending themselves to a rigorous analysis which would be less complicated than the corresponding case involving anisotropic fibres.

Acknowledgements

We wish to express our gratitude to Mr A. L. Rickards, Mr G. L. Wicker and Dr G. H. Wostenholm for various forms of practical assistance, to Dr W. C. Streib for helpful correspondence and to the Science Research Council for a CAPS award received by one of us (C.H.).

References

1. A. A. HODGSON, "Fibrous Silicates", Lecture Series, 1965, No. 4 (Royal Institute of Chemistry, London, 1966).
2. S. SPEIL and J. P. LEINEWEBER, *Environmental Research* 2 (1969) 166.
3. C. HARWOOD, G. H. WOSTENHOLM, B. YATES and D. V. BADAMI, *J. Polymer Sci. Polymer Phys. ed.* **16** (1978) 759.
4. E. J. W. WHITTAKER, *Acta Cryst.* 6 (1953) 747.
5. *Idem, ibid.* 8 (1955) 571.
6. K. YADA, *ibid.* 23 (1967) 704.
7. F. L. PUNDSACK, *J. Phys. Chem.* **60** (1956) 361.
8. *Idem, ibid.* 65 (1961) 30.
9. B. T. KELLY, B. A. McCALLA, G. H. WOSTENHOLM and B. YATES, *J. Nucl. Mater.* **61** (1976) 221.
10. E. P. PLUEDDEMANN, "Composite Materials", Vol. 6 (Academic Press, London, 1974) p. 173.
11. W. C. STREIB, private communication.
12. A. C. BAILEY and B. YATES, *J. Appl. Phys.* **41** (1970) 5088.
13. B. YATES, M. J. OVERY and O. PIRGON, *Phil. Mag.* **32** (1975) 847.
14. T. H. K. BARRON, *Ann. Phys. N.Y.* **1** (1957) 77.
15. M. BLACKMAN, *Phil. Mag.* **3** (1958) 831.
16. E. G. KING, R. BARANY, W. W. WELLER and L. B. PANKRATZ, U.S. Bureau of Mines Rep. No. 6962 (1967).
17. W. GÖTZE and F. WINKLER, *Deutsche Textiltechnik* **18** (1968) 297.
18. R. W. MUNN, *Adv. Phys.* 18 (1969) 515.
19. N. J. CHAMBERLAIN, BAC Rep. No. SON (P) 33 (1968).
20. R. A. SCHAPERY, *J. Comp. Mater.* 2 (1968) 380.
21. W. SCHNEIDER, *Kunststoffe* **61** (1971) 23.
22. J. C. HALPIN and N. J. PAGANO, AFML-TR-68-395 (1969).
23. N. J. PAGANO, *J. Comp. Mater.* 8 (1974) 310.
24. K. F. ROGERS, L. N. PHILLIPS, D. M. KINGSTON-LEE, B. YATES, M. J. OVERY, J. P. SARGENT and B. A. McCALLA, *J. Mater. Sci.* **12** (1977) 718.
25. B. YATES, M. J. OVERY, J. P. SARGENT, B. A. McCALLA, D. M. KINSTON-LEE, L. N. PHILLIPS and K. F. ROGERS, *ibid.* **13** (1978) 433.

26. J. C. HALPIN and N. J. PAGANO, *J. Comp. Mater.* 3 (1969) 720.
27. J. C. HALPIN, *ibid.* 3 (1969) 732.
28. J. C. HALPIN, K. JERINE and J. M. WHITNEY, *ibid.* 5 (1971) 36.
29. R. M. CHRISTENSEN and F. M. WAALS, *ibid* 6 (1972) 518.
30. R. M. CHRISTENSEN, *Int. J. Solids Structures* 12 (1976) 537.
Received 14 July and accepted 6 September 1978.